Chemical-genetic inhibition of a sensitized mutant myosin Vb demonstrates a role in peripheral-pericentriolar membrane traffic

D. William Provance, Jr.*, Christopher R. Gourley*, Colleen M. Silan*, L. C. Cameron†, Kevan M. Shokat‡, James R. Goldenring§, Kavita Shah¶, Peter G. Gillespie‖, and John A. Mercer*,**

*McLaughlin Research Institute, Great Falls, MT 59405; †Universidade Federal do Estado do Rio de Janeiro, Universidade Estácio de Sá, Universidade Castelo Branco, CEP 22290-280, Rio de Janeiro, Brazil; ‡Department of Cellular and Molecular Pharmacology, University of California, San Francisco, CA 94143; §Departments of Surgery and Cell and Developmental Biology, Vanderbilt University School of Medicine and Nashville Veterans Affairs Medical Center, Nashville, TN 37235; ¶Genomics Institute of the Novartis Research Foundation, San Diego, CA 92121; and ‖Oregon Hearing Research Center, Oregon Health and Science University, and Vollum Institute, Portland, OR 97239

Edited by James A. Spudich, Stanford University School of Medicine, Stanford, CA, and approved December 10, 2003 (received for review September 12, 2003)

Selective, *in situ* inhibition of individual unconventional myosins is a powerful approach to determine their specific physiological functions. Here, we report the engineering of a myosin Vb mutant that still hydrolyzes ATP, yet is selectively sensitized to an N^6-substituted ADP analog that inhibits its activity, causing it to remain tightly bound to actin. Inhibition of the sensitized mutant causes inhibition of accumulation of transferrin in the cytoplasm and increases levels of plasma-membrane transferrin receptor, suggesting that myosin Vb functions in traffic between peripheral and pericentrosomal compartments.

The characterization of the specific cellular functions of unconventional myosins has lagged behind their identification for several reasons. First, redundancy occurs within myosin families. Second, all myosins identified to date hydrolyze ATP, making most ADP and ATP analogs ineffective for identifying individual functions of molecular motors. Third, a popular approach is the overexpression of carboxy-terminal tail domains of these proteins; however, this approach does not detect any functions dependent on prior positioning by the motor domain and can yield nonspecific effects from overexpression. Fourth, although genetic-ablation approaches are very powerful, null mutants often only illuminate the initial process for which a given motor is required during development, often precluding the study of later physiological functions.

Specific, acute inhibition of the activity of individual molecular motors *in situ* is an ideal approach for determining specific functions. We have used a chemical-genetic strategy, first developed for kinases (1), that achieves selectivity, specificity, and temporal control. We started by examining the crystal structure of the ATP-binding pocket of a myosin (2). By site-directed mutagenesis of the tyrosine codon found in close proximity to the N^6 position of the bound nucleotide, we enlarged the ATP-binding pocket. Our goal was to inhibit the sensitized myosin with a specific N^6-modified ADP analog that is too bulky to affect its wild-type counterpart, causing the mutant myosin to bind tightly to actin. At the same time, the mutant should hydrolyze cellular ATP and function normally in the absence of analog. The acute cellular application of the inhibitor by microinjection or dialysis allows the use of short timescales and micromolar concentrations of an analog that may have effects on other cellular functions during longer treatments. This method has been successful (both *in vitro* and *in vivo*) with another unconventional myosin, myosin 1c (myosin I beta) (3, 4). A similar strategy also has been applied to kinesin (5) and several small G proteins (K.S., unpublished data).

We describe the use of this approach to study a member of the myosin V family (6–8). The family has three members in mammals: myosin Va (*dilute*) (9), myosin Vb (myr 6; ref. 10), and myosin Vc (11). These myosins have been implicated in human and murine genetic disease, synaptic transmission, secretion, and plasma membrane recycling (12–14). Myosin Vb is an attractive subject because it has several apparent roles in membrane transport, including recycling of transferrin and its receptor (15), recycling of the M4 muscarinic acetylcholine receptor (16), and other potential functions, given its interactions with GTP-bound members of the Rab11 family (15).

We have identified an ADP analog, N^6-(2-phenylethyl)-ADP (PE-ADP), that selectively induces binding of the Y119G mutant of myosin Vb to actin *in vitro*. We have shown that selective inhibition of Y119G myosin Vb by PE-ADP in HeLa cells leads to inhibition of transferrin uptake. We also found that levels of plasma-membrane transferrin receptor are increased by myosin Vb inhibition. These results are the converse of those obtained by using overexpression of dominant-negative myosin Vb tail fragments (15). Finally, we present a model that reconciles these apparent disparities. Our data show that chemical genetics provides a powerful approach that complements other methods for studying the functions of molecular motors.

Methods

Expression Constructs. The full-length rat myosin Vb coding sequence (10, 15) (Fig. 1*C*) was transferred to the pUni/V5-His-TOPO vector (Invitrogen) and mutagenized (QuikChange, Stratagene) to code for glycine instead of tyrosine at position 119 (Y119G). The mutagenesis also introduced a *Pvu*II site that enabled identification of wild-type and mutant constructs and transcripts. This insert was shuttled to pCDNA3.1-E (Invitrogen). We also made truncated versions of both myosin Vb constructs (Fig. 1*B*), leaving only the head domain and a single IQ motif, but retaining the C-terminal V5 and $His_{(6)}$ tags.

Expression of Recombinant Myosin Vb. Madin–Darby canine kidney and HeLa cells were cultured as described (15). Cells were transfected with myosin Vb constructs by using Lipofectamine 2000 (Invitrogen) and allowed to express for 24 h before lysis (Madin–Darby canine kidney) or selected in G418 to produce lines for microinjection (HeLa). Myosin Vb was purified from Madin–Darby canine kidney lysates by the protocol used for myosin 1c (3) with the following modifications. Complete EDTA-free protease inhibitor mixture (Roche Diagnostics) was added to the lysis buffer and cells were lysed by 40 passes in a ball-bearing cell cracker (15-μm clearance). Ni^{2+}-nitriloacetic

This paper was submitted directly (Track II) to the PNAS office.

Abbreviations: PE-ADP, N^6-(2-phenylethyl)-ADP; TfR, transferrin receptor.

**To whom correspondence should be addressed at: McLaughlin Research Institute, 1520 23rd Street South, Great Falls, MT 59405. E-mail: umbjm@montana.edu.

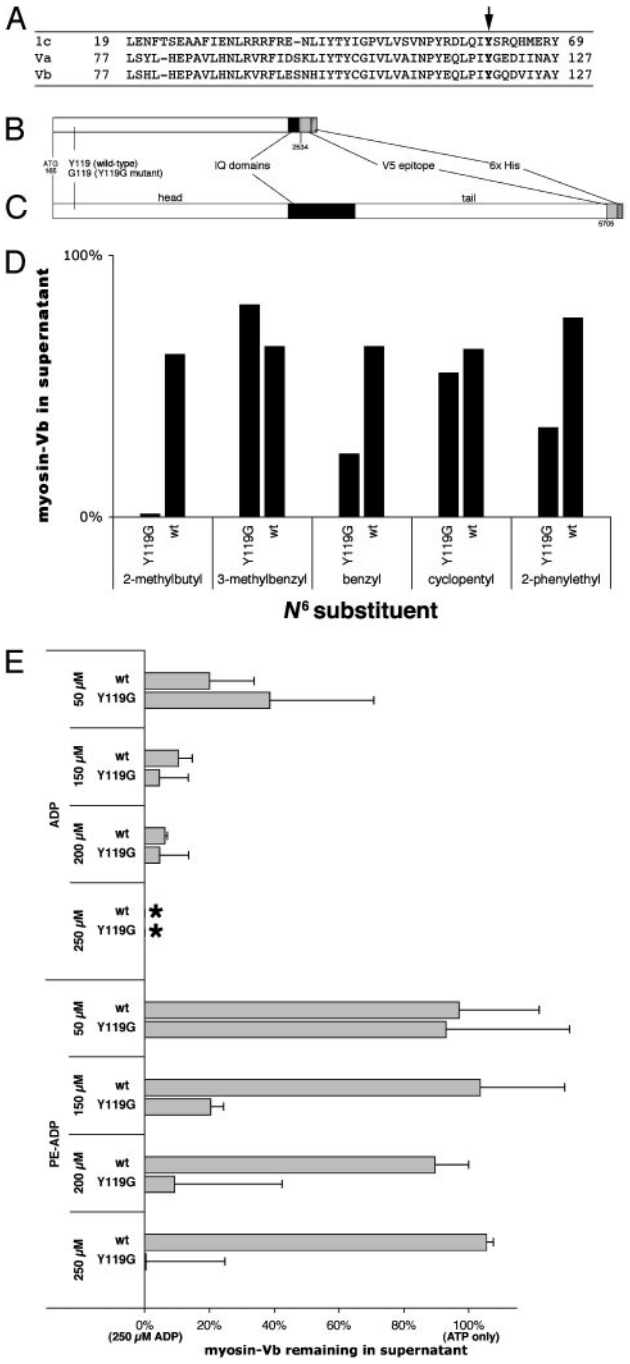

Fig. 1. Characterization of mutant and wild-type myosin Vb. (*A*) Sequence alignment of myosin 1c, myosin Va, and myosin Vb showing conserved tyrosine (arrow). (*B*) Diagram of truncated myosin Vb insert. (*C*) Diagram of full-length myosin Vb insert. Numbers below the diagrams refer to nucleotides from GenBank accession no. U60416 (10). (*D*) Effects of 100 μM concentrations of five ADP analogs. (*E*) Effects of ADP and PE-ADP on myosin/ATP/actin-binding equilibria for truncated wild-type (wt) and mutant (Y119G) myosin Vb. Cosedimentation data are plotted as the proportion of myosin remaining in the supernatant relative to the data for 100 μM ATP only (100%) and the proportion remaining for 100 μM ATP plus 250 μM ADP (0%; *) on the same blot. Error bars represent standard deviations. A representative Western blot is shown in Fig. 6, which is published as supporting information on the PNAS web site.

acid-agarose (Sigma) was batch-loaded with the lysates for 45 min on ice. The column was washed successively with wash buffer containing 4 mM Mg^{2+}-ATP and 50 mM imidazole and finally with wash buffer alone. Imidazole in the elution buffer was increased to 150 mM.

Cosedimentation Assays. Actin cosedimentation assays were performed by mixing the eluates described above with 10 μM phalloidin-stabilized F-actin in ultracentrifuge tubes on ice in the buffer used for myosin 1c (3). Mixtures of nucleotides (with 100 μM Mg^{2+}-ATP in all samples) were added on the sides of the tubes. Centrifugation was performed at 186,000 $\times$ *g* for 20 min. Supernatants and pellets were solubilized, separated by SDS/PAGE, and blotted, and recombinant myosin Vb was detected by chemiluminescence by using anti-V5 (see below), detected, and quantitated with a VersaDoc 5000 (Bio-Rad).

Microinjection. ADP analogs (2.5 mM) were injected into the cytoplasm of HeLa cells with a Harvard Apparatus PLI-100 at 8–20 kPa. The injection buffer contained 150 mM KCl, 2 mg/ml fixable Cascade Blue dextran (Molecular Probes), 10 mM ATP, and 2 mM Hepes (pH 7.0). Cells were allowed to recover for 5 min, and Alexa 546-transferrin (Molecular Probes) was added to the medium at 10 μg/ml for 10 min in some experiments.

Antibodies. Myosin Vb was detected with monoclonal anti-V5 (Invitrogen). Transferrin receptor was detected with monoclonal anti-human CD71 (Cymbus Bioscience, Southhampton, U.K.). Alexa 488-goat anti-mouse IgG was purchased from Molecular Probes. For Western blots, horseradish peroxidase-conjugated goat anti-mouse IgG (Santa Cruz Biotechnology) was used as secondary antibody and detected with SuperSignal West Pico substrate (Pierce). In all cases, the background fluorescence in an area without cells was subtracted.

Imaging. Fluorescence micrographs were acquired with a Nikon TE-2000E equipped with a Q57 camera (Roper Scientific, Trenton, NJ). Exposure times were kept constant within each experiment. Fluorescence per unit area was quantified after background subtraction with METAMORPH software (Universal Imaging, Media, PA).

Results

Myosin Vb Chemical-Genetic Strategy. Both myosin Va (9) and myosin Vb (10) have a conserved tyrosine residue at position 119 (Fig. 1*A*), corresponding to the myosin 1c Y61 residue mutated to engineer a sensitized mutant (3). We therefore mutagenized myosin Vb to produce the homologous mutant, Y119G. Both mutant and wild-type myosin Vb were initially expressed in a baculovirus system, but expression levels were inadequate (data not shown). We circumvented this problem by expressing wild-type and mutant constructs lacking the tail domain (Fig. 1*B*) in Madin–Darby canine kidney cells. Because the construct lacks the coiled–coil domain, it should not dimerize. The same truncation of chicken myosin Va has enzymatic activity (17, 18).

Screening for Selective ADP Analog Inhibitors by Actin Cosedimentation. Because screening of analogs by ATPase assays and actin cosedimentation gave similar results in our earlier work (3) and ATPase assays with myosin V are complicated by rapid inhibition of myosin V by the ADP produced (19), we chose actin cosedimentation for screening because it is a better *in vitro* model for the desired effect in the cell. We determined the effects of five ADP analogs on the myosin/ATP/actin-binding equilibrium of truncated Y119G mutant myosin Vb, with its wild-type counterpart as a control. Phalloidin-stabilized actin and truncated myosin Vb were mixed with 100 μM ATP plus a 100 μM concentration of each analog and immediately sedimented. Surprisingly, three of the five analogs were selective in their induction of actin binding (Fig. 1*D*).

Based on the HeLa cell screen described in the next section,

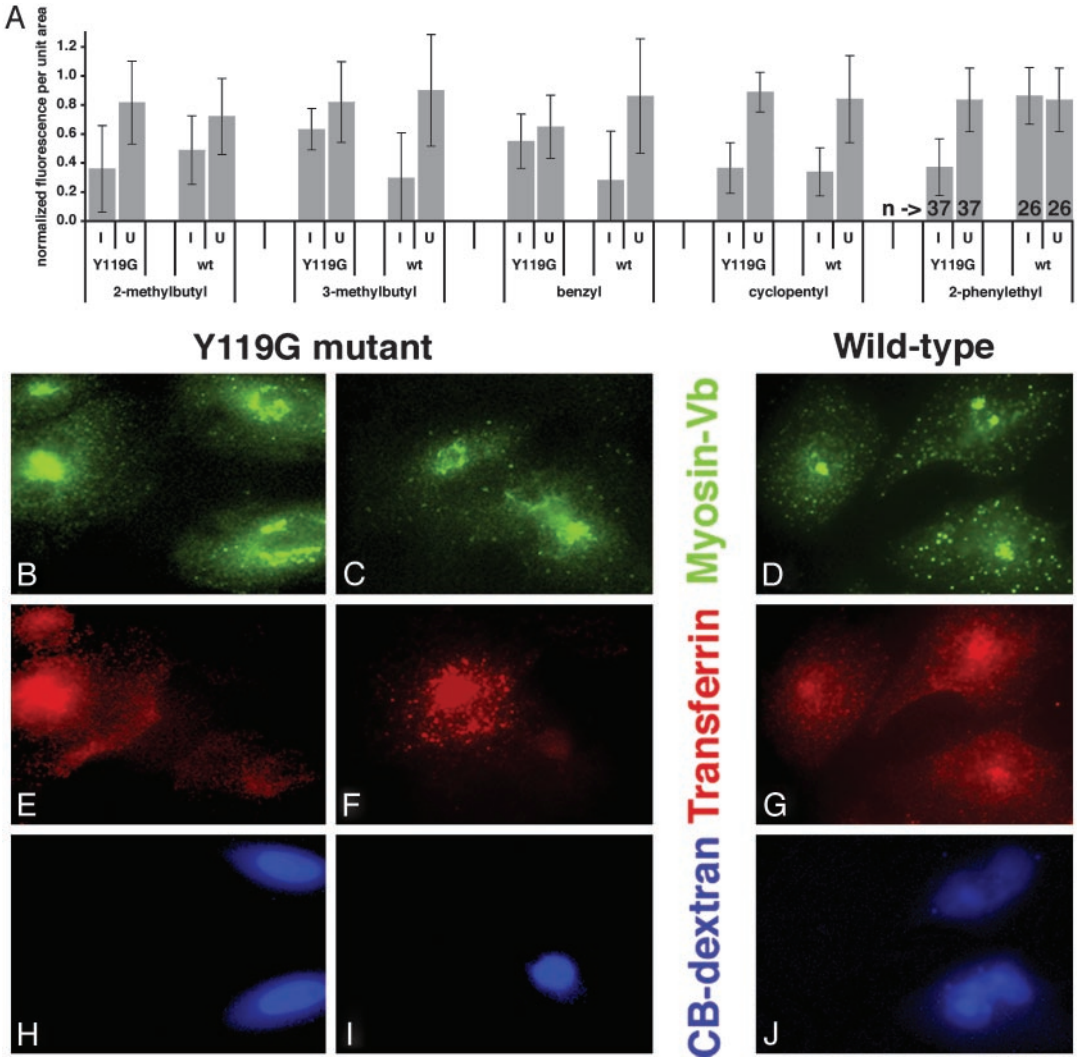

Fig. 2. Screen of ADP analogs for the ability to alter transferrin uptake in HeLa cells expressing sensitized myosin Vb. Cells expressing mutant or wild-type myosin Vb were microinjected with Cascade Blue dextran and a 2.5 mM concentration of each ADP analog. Cells were then incubated with fluorescent transferrin. (*A*) Plots of cytoplasmic fluorescence per unit area. Because fluorescence levels varied between coverslips and experiments, fluorescence measurements were normalized to the level of the brightest cell in the same field. Error bars represent standard deviation. I, injected; U, uninjected; Y119G, cells expressing sensitized mutant myosin Vb; wt, cells expressing control wild-type myosin Vb; bottom line, N^6 substituent. Numbers of cells are shown for the PE-ADP groups at the far right. (*B–J*) Representative cells from the PE-ADP experiment. HeLa cells expressing mutant (*B*, *C*, *E*, *F*, *H*, and *I*) and control wild-type myosin Vb (*D*, *G*, and *J*) were cultured on coverslips. Cells were imaged for anti-V5 to detect myosin Vb (*B–D*), Alexa 546-transferrin (*E–G*), and Cascade Blue, which accumulates in nuclei, to identify injected cells (*H–J*). The tubulovesicular distribution of mutant myosin Vb in injected cells (*B*, two cells on right) was observed in most, but not all, cases. (Bar = 10 μm.) Additional cells are shown in Fig. 7, which is published as supporting information on the PNAS web site.

PE-ADP was chosen for more detailed study. The results of actin cosedimentation in the presence of ADP and PE-ADP are shown in Fig. 1*E*. The sensitivity of Y119G mutant myosin Vb to ADP was somewhat less than that of wild-type myosin Vb. The effect of PE-ADP, however, was dramatically different; wild-type myosin Vb was insensitive to PE-ADP at concentrations up to 500 μM (not shown; 118 ± 11%), whereas the sensitivity of mutant myosin Vb to PE-ADP was similar to its sensitivity to ADP.

Screening for Specific and Selective Inhibitors During Transferrin Trafficking in HeLa Cells. To determine the specificity of the five ADP analogs in a cellular context with full-length myosin Vb, we expressed full-length wild-type and Y119G (Fig. 1*C*) in HeLa cells by transfection and selection with 100 μg/ml G418. These cell lines, used in all experiments described below, were indistinguishable from untransfected control cells in their uptake and clearing of fluorescent transferrin at 5, 10, 20, and 40 min of exposure (data not shown). Higher expression levels of myosin Vb caused a decrease in transferrin uptake (data not shown).

We microinjected the cell lines (two independently derived mutant and two wild-type) with the five ADP analogs used in the actin cosedimentation assays. Assuming an injection volume of 6–10% of the cytoplasmic volume, the injections should provide a cytoplasmic concentration of ≈150–250 μM for each ADP analog. The raw average cytoplasmic transferrin fluorescence per pixel was used as a measure of transferrin uptake. This fluorescence was normalized to that of the brightest cell in the same field and plotted (Fig. 2*A*).

N^6-(2-methylbutyl)-ADP inhibited transferrin uptake in cells expressing the mutant myosin Vb, but inhibition also was observed in control cells expressing wild-type myosin Vb. Both N^6-(3-methylbenzyl)- and N^6-(2-benzyl)-ADP caused more inhibition of transferrin uptake in wild-type controls than in cells expressing the mutant myosin. Significant inhibition of trans-

ferrin uptake was observed in cells expressing both wild-type and Y119G myosin Vb after injection with N^6-(cyclopentyl)-ADP.

Of the five analogs, only PE-ADP was both specific and selective in this situation. Whereas the graphs in Fig. 2*A* represent normalized data, analyses of the nonnormalized data by other methods also show a significant effect. When the four PE-ADP groups were compared with each other by unpaired, two-tailed, heteroscedastic *t* tests, the only significant differences found were between the group of injected cells expressing mutant myosin Vb and all three negative control groups. ANOVA for all four groups gave a *P* value of 0.008.

Representative micrographs from the PE-ADP injections are shown in Fig. 2 *B–J*, and additional cells are shown in Fig. 8, which is published as supporting information on the PNAS web site. Fig. 2 *D* and *E* demonstrate that the injected cells have reduced levels of cytoplasmic transferrin, and Fig. 2 *A* and *B* show localization of the exogenous myosin Vb in tubulovesicular structures in injected cells. This morphology is similar to that observed after overexpression of a GFP fusion with the C-terminal 65 amino acids of Rab11-FIP2, which also colocalizes with Rab11a (20).The absence of effects in cells expressing wild-type control myosin Vb (Fig. 2 *D*, *G*, and *J*) serves as a coisogenic control that isolates the effects of a single amino acid difference, a control for nonspecific effects of microinjection, and a control for any effects of the analog on any other cellular proteins involved in transferrin endocytosis and trafficking during this short interval.

Because an effect on uptake of transferrin would preclude observation of the hypothesized role of myosin Vb in transport from pericentrosomal compartments to the plasma membrane (15), we performed a more direct test by performing PE-ADP injection after loading with fluorescent transferrin. Surprisingly, we observed no effect (Fig. 9, which is published as supporting information on the PNAS web site). This also provides a negative control for nonspecific effects such as actin crosslinking.

The Inhibited Mutant Myosin Vb Does Not Block Other Myosins Involved in Transferrin Trafficking by Binding to Actin. One hypothesis explaining these data is that the mutant myosin Vb, arrested in a rigor state by PE-ADP, is blocking other myosins that are actively mediating transport. We have tested this hypothesis by injecting PE-ADP into cells expressing truncated Y119G myosin Vb lacking the tail domain (Fig. 1*B*), for which the induction of actin binding by PE-ADP was similar to that of full-length myosin Vb (Fig. 9). Average expression levels of the truncated myosin Vb were higher that those observed for full-length myosin Vb. Also, because the truncated control construct lacks a tail domain, it has a more extensive colocalization with actin. Using this control, we observed no difference (*t* test, $P = 0.61$) in transferrin uptake between uninjected and injected cells, as well as no correlation between the amount of tailless mutant myosin Vb expressed and transferrin uptake in injected cells (Fig. 3).

Inhibition of Sensitized Mutant Myosin Vb Increases Amounts of Transferrin Receptor (TfR) on the Plasma Membrane. Multiple steps in transferrin endocytosis and trafficking could be inhibited by our specific inhibition of myosin Vb. To begin to discriminate among these steps, we hypothesized that myosin Vb is engaged with actin during an early, peripheral step in TfR recycling. To test this hypothesis, we microinjected transfected, serum-starved HeLa cells with PE-ADP and detected only plasma-membrane TfR by immunofluorescence without permeabilizing the cells after fixation. Representative cells are shown in Fig. 4. Cells expressing the Y119G mutant and microinjected with PE-ADP exhibited significantly higher levels of plasma-membrane TfR than did uninjected cells expressing the mutant. The effect was specific for the mutant, because no difference occurred between injected and uninjected control cells expressing wild-type myosin

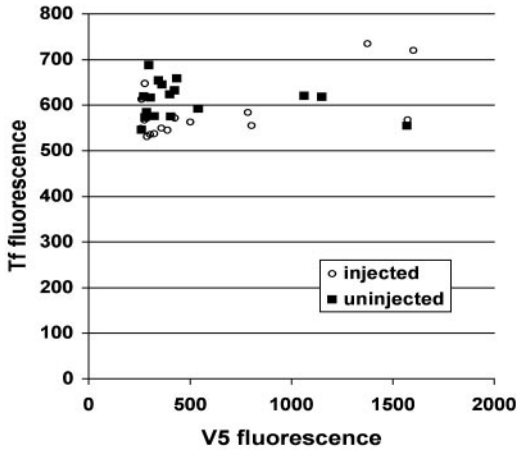

Fig. 3. Inhibition of a truncated, tailless Y119G myosin Vb fragment has no effect on transferrin uptake. HeLa cells expressing truncated mutant myosin Vb (Fig. 1*B*) were microinjected for 2 min with PE-ADP and Cascade Blue dextran, allowed to recover for 5 min, and incubated with Alexa 546-transferrin for 10 min. V5 fluorescence, a measure of expression levels of the myosin Vb construct, is plotted on the *x* axis, and transferrin fluorescence is plotted on the *y* axis. ○, values from injected cells; ■, values from uninjected cells.

Vb. By *t* tests, the raw average TfR signals per unit area were significantly different between injected (720 ± 178, mean ± SD) and uninjected (203 ± 78) cells expressing the mutant ($P = 5 \times 10^{-10}$), but not between injected (369 ± 209) and uninjected (284 ± 137) cells expressing wild-type myosin Vb ($P = 0.10$). Plasma-membrane TfR levels in injected cells expressing the mutant also were significantly different from those of injected cells expressing the wild-type myosin Vb ($P = 1 \times 10^{-5}$). A similar increase in plasma-membrane TfR was observed after only 1 min of recovery after microinjection and in the presence of serum.

Discussion

In this report, we demonstrate selective and specific inhibition of myosin Vb by using a chemical-genetic strategy. This inhibition prevented accumulation of transferrin in pericentriolar compartments of HeLa cells, consistent with a role for myosin Vb in trafficking of transferrin and its receptor in transitions between peripheral and pericentriolar membrane compartments. This strategy is especially powerful because it provides multiple negative controls that cannot be used with other methods. The primary negative control, cells transfected with a wild-type myosin Vb

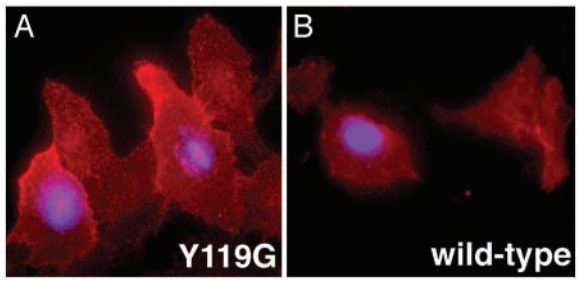

Fig. 4. Inhibition of mutant myosin Vb increases levels of plasma-membrane transferrin receptor. HeLa cells expressing sensitized mutant (*A*) and wild-type (*B*) Myosin Vb were serum-starved for 30 min and some were injected (blue nuclei) with PE-ADP and Cascade Blue dextran. Cells were allowed to recover for 10 min at 37°C before fixation. Surface TfR was detected by indirect immunofluorescence.

CELL BIOLOGY

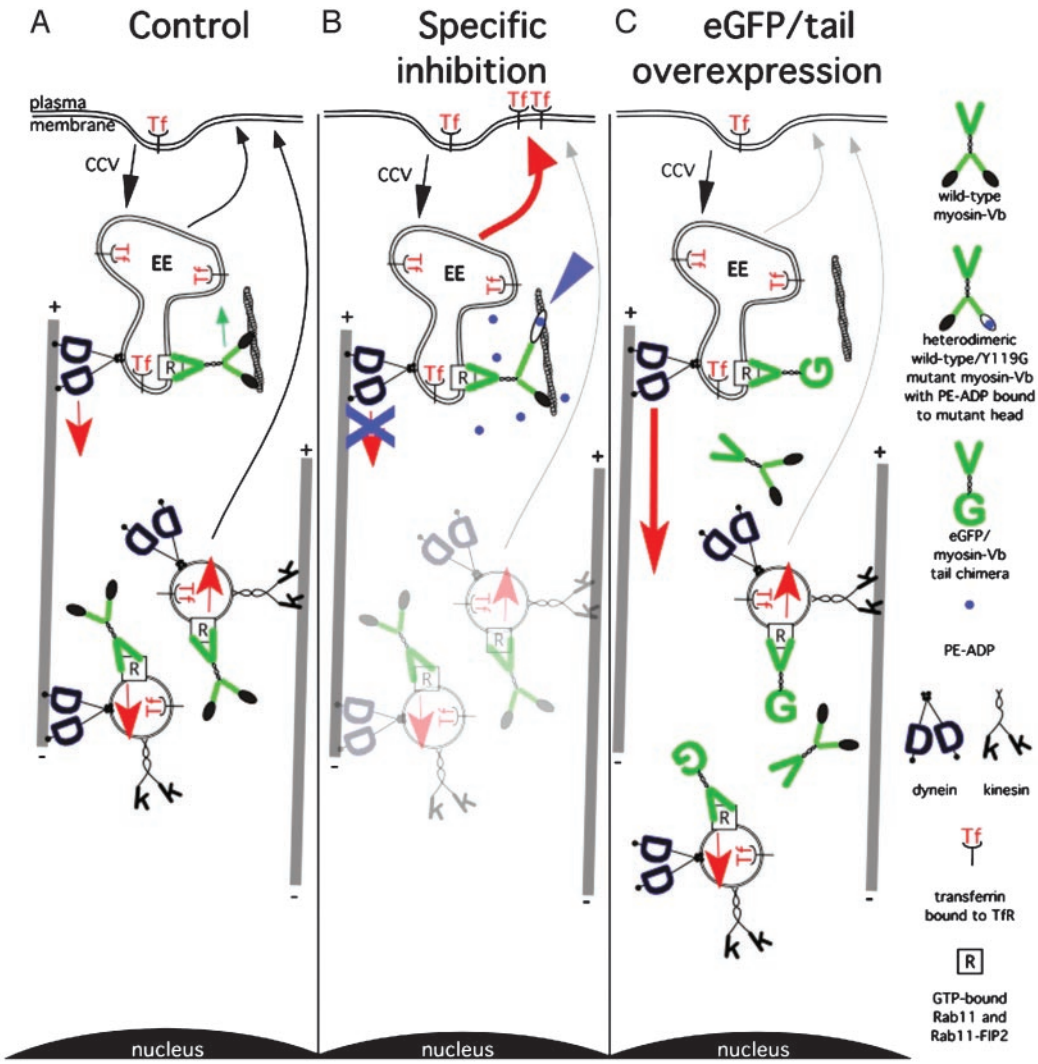

Fig. 5. Model reconciling results from chemical-genetic and tail-fragment approaches to inactivating myosin Vb during transferrin uptake in HeLa cells. (*A*) Normal state in which myosin Vb antagonizes retrograde budding of vesicles from early endosomes (EE) along microtubules, after which it is distributed within the cytoplasm by equilibrium between anterograde and retrograde microtubule-based motility. (*B*) Inhibition of mutant myosin Vb by PE-ADP prevents retrograde exit from the early endosome, shunting transferrin and TfR into peripheral recycling pathways (red arrow). (*C*) Overexpression of the enhanced GFP/myosin Vb tail (15) prevents this antagonism, causing pericentriolar accumulation of endocytosed transferrin. Late endosomes, pericentriolar recycling vesicles, lysosomes, Golgi complex, and intermediate membrane compartments are omitted.

construct, does triple duty as a coisogenic control that isolates the effects of a single amino acid difference, as a control for nonspecific effects of microinjection, and as a control demonstrating the absence of effects of the analog on any other relevant cellular functions during the short experimental interval. To control for indirect effects on other myosins whose paths along actin may be blocked by the bound mutant myosin Vb, we expressed and inhibited a truncated, tailless Y119G myosin Vb. Our data also show that *in vitro* assays can identify selective analogs, but the effects of these analogs on other cellular functions vary, suggesting that different inhibitors are required for studying an individual myosin in different experimental systems.

Based on dominant-negative tail-fragment results (15), we chose fluorescent transferrin uptake as our system for screening candidate ADP analogs. We found that PE-ADP selectively and specifically inhibited transferrin uptake and had no effect on clearing in HeLa cells expressing the Y119G mutant myosin Vb. This result was unexpected, because overexpression of a myosin Vb tail/enhanced GFP chimera causes the converse phenotype: pericentriolar accumulation of endocytosed transferrin, with no effect on uptake (15). This disparity can be reconciled because the inhibition is accomplished in two different ways: overexpression of tail fragments prevents binding of the myosin to its cargo, disengaging it from actin, whereas the chemical-genetic approach tightly binds the myosin to actin. This difference allows the reconciliation of both sets of data in a modification of the "tug-of-war" model proposed for the role of myosin Va in melanosome transport (21). In this model, retrograde microtubule-based transport by dynein antagonizes and surpasses anterograde transport by kinesin, whereas a myosin V makes a net contribution to anterograde transport by capturing or tethering melanosomes in the periphery. Similar models have been proposed for chromaffin cell exocytosis (22) and for vesicle transport in neurons (23) and sea urchin eggs (24).

In our modification, myosin Vb negatively regulates the retrograde budding of vesicles from peripheral compartments (illustrated here as early endosomes) driven by dynein (Fig. 5*A*). The role of myosin Vb in our model is analogous to that of myosin 1c in slipping adaptation in hair cells (4). After the tubule detaches and becomes a vesicle, some myosin Vb is transported

as a passenger to pericentriolar recycling compartments, accounting for its presence there. When PE-ADP causes sensitized mutant myosin Vb to bind tightly to actin (Fig. 5*B*, blue arrowhead), it can no longer slip, inhibiting retrograde budding or transport. This inhibition should occur even for heterodimers of mutant and wild-type myosin Vb. With multiple myosin Vbs on an organelle, a single inhibited mutant head tightly bound to actin may be sufficient to inhibit motility. We hypothesize that this inhibition causes transferrin and its receptor to be shunted into peripheral recycling pathways (red arrow, Fig. 5*B*), accounting for the increased amount of TfR on the plasma membrane observed on myosin Vb inhibition (Fig. 4). This model also is consistent with our observation that overexpression of myosin Vb caused inhibition of transferrin uptake. With overexpression of the tail (Fig. 5*C*), endogenous myosin Vb is displaced, preventing its antagonism of dynein. This increases retrograde transport of transferrin (Fig. 5*C*, thick red arrow), leading to accumulation of the tail fragment, transferrin, and Rab11a in pericentrosomal compartments. The observation that nocodazole treatment caused the partial dispersion of the pericentrosomal aggregation caused by the tail fragment (15) also is consistent with this model.

Because myosin Vb apparently only interacts with GTP-bound Rab11a (15), our model is compatible with the results of Sabatini's group (25), who concluded that hydrolysis of GTP by Rab11a is necessary for anterograde transport of transferrin from pericentriolar compartments to the plasma membrane. Expression of a C-terminal dominant-negative fragment of Rab11-FIP2, which interacts with both Rab11 and myosin Vb (26), in HeLa cells caused transferrin to accumulate in tubular structures whose morphology depended on microtubule integrity (20). A similar phenotype was observed after expression of a dominant-negative mutant Rab11 in HeLa cells (27), and both resemble the tubulovesicular phenotype we often observed on inhibition of Y119G myosin Vb (Fig. 2 *B* and *C*).

The interaction between myosin Va and kinesin (28) provides support for a second model (not shown) in which myosin Vb and a kinesin interact directly or use the same receptor on some organelles, presumably Rab11 and its partners (26, 29, 30). In this model, overexpression of the myosin Vb tail fragment inhibits anterograde transport by displacing kinesin from its cargo. The chemical-genetic approach, however, should neither inhibit transferrin clearing in cells preloaded with transferrin (Fig. 8) nor displace kinesin from organelles, because the Y119G mutant myosin Vb is expressed at only 20–30% of endogenous levels.

The two data sets can be reconciled in several other ways: (*i*) Myosin Vb may have a function during endocytosis itself, consistent with the association of Rab11-FIP2 with the α-adaptin subunit of AP-2 complexes (31); (*ii*) myosin V may be cooperating with other myosins, but is not required; (*iii*) a relative deficit of the enhanced GFP/myosin Vb tail chimera in the cortex of the cell could be caused by its accumulation in the pericentriolar region; or (*iv*) the concentration of the enhanced GFP/myosin Vb tail chimera in cortical actin may be insufficient to displace endogenous myosin Vb, because it lacks the positioning provided by the head domain. In support of this interpretation, the localization of full-length myosin 1b was not explained by either head or tail constructs alone (32). All of these alternatives also account for the increase in plasma-membrane TfR we observed after inhibition of Y119G myosin Vb.

In summary, our results suggest an important role for myosin Vb during trafficking of transferrin and its receptor. The dramatic differences between our data and those obtained with other approaches suggest that the chemical-genetic method provides more direct, acute assays of myosin function that will drive refinements to current models. The advantages of our approach include the elimination of nonspecific effects of overexpression, limiting the effects of inhibition to situations in which the myosin is engaged with actin and the ability to examine the function of full-length mutant myosins that function normally until the acute application of inhibitor. Moreover, chemical-genetic inhibition, unlike other methods, can perturb myosin function in the short term (1–20 min). Our success in applying the chemical-genetic approach to both myosin 1c and myosin Vb suggests that this approach has great potential for all myosins.

We thank Enrique De La Cruz for advice on ATPase and actin cosedimentation assays and George Carlson, John Bermingham, Pin-Xian Xu, Ryan Karcher, and Rajeev Kumar for helpful discussions. Equipment was provided by a grant from the M. J. Murdock Charitable Trust (Vancouver, WA). This research was supported by McLaughlin Research Institute funds and National Institutes of Health Grants DC03279 (to J.A.M. and P.G.G.), EB001987 (to K.M.S.), and DK48370 and DK38063 (to J.R.G.) C.R.G. was supported by National Institutes of Health COBRE Grant RR015583.

1. Bishop, A. C., Buzko, O. & Shokat, K. M. (2001) *Trends Cell Biol.* **11,** 167–172.
2. Gulick, A. M., Bauer, C. B., Thoden, J. B. & Rayment, I. (1997) *Biochemistry* **36,** 11619–11628.
3. Gillespie, P. G., Gillespie, S. K. H., Mercer, J. A., Shah, K. & Shokat, K. M. (1999) *J. Biol. Chem.* **274,** 31373–31381.
4. Holt, J. R., Gillespie, S. K. H., Provance, D. W., Shah, K., Shokat, K. M., Corey, D. P., Mercer, J. A. & Gillespie, P. G. (2002) *Cell* **108,** 371–381.
5. Kapoor, T. M. & Mitchison, T. J. (1999) *Proc. Natl. Acad. Sci. USA* **96,** 9106–9111.
6. Langford, G. M. & Molyneaux, B. J. (1998) *Brain Res. Brain Res. Rev.* **28,** 1–8.
7. Provance, D. W. & Mercer, J. A. (1999) *Cell. Mol. Life Sci.* **56,** 233–242.
8. Reck-Peterson, S. L., Provance, D. W., Mooseker, M. S. & Mercer, J. A. (2000) *Biochim. Biophys. Acta* **1496,** 36–51.
9. Mercer, J. A., Seperack, P. K., Strobel, M. C., Copeland, N. G. & Jenkins, N. A. (1991) *Nature* **349,** 709–713.
10. Zhao, L. P., Koslovsky, J. S., Reinhard, J., Bähler, M., Witt, A. E., Provance, D. W. & Mercer, J. A. (1996) *Proc. Natl. Acad. Sci. USA* **93,** 10826–10831.
11. Rodriguez, O. C. & Cheney, R. E. (2002) *J. Cell Sci.* **115,** 991–1004.
12. Hasson, T. & Mooseker, M. S. (1996) *J. Biol. Chem.* **271,** 16431–16434.
13. Mooseker, M. S. & Cheney, R. E. (1995) *Annu. Rev. Cell Dev. Biol.* **11,** 633–675.
14. Titus, M. A. (1997) *Trends Cell Biol.* **7,** 119–123.
15. Lapierre, L. A., Kumar, R., Hales, C. M., Navarre, J., Bhartur, S. G., Burnette, J. O., Provance, D. W., Jr., Mercer, J. A., Bahler, M. & Goldenring, J. R. (2001) *Mol. Biol. Cell* **12,** 1843–1857.
16. Volpicelli, L. A., Lah, J. J., Fang, G., Goldenring, J. R. & Levey, A. I. (2002) *J. Neurosci.* **22,** 9776–9784.
17. De La Cruz, E. M., Wells, A. L., Rosenfeld, S. S., Ostap, E. M. & Sweeney, H. L. (1999) *Proc. Natl. Acad. Sci. USA* **96,** 13726–13731.
18. De La Cruz, E. M., Wells, A. L., Sweeney, H. L. & Ostap, E. M. (2000) *Biochemistry* **39,** 14196–14202.
19. De La Cruz, E. M., Sweeney, H. L. & Ostap, E. M. (2000) *Biophys. J.* **79,** 1524–1529.
20. Lindsay, A. J. & McCaffrey, M. W. (2002) *J. Biol. Chem.* **277,** 27193–27199.
21. Gross, S. P., Tuma, M. C., Deacon, S. W., Serpinskaya, A. S., Reilein, A. R. & Gelfand, V. I. (2002) *J. Cell Biol.* **156,** 855–865.
22. Rosé, S. D., Lejen, T., Casaletti, L., Larson, R. E., Pene, T. D. & Trifaró, J. M. (2003) *J. Neurochem.* **85,** 287–298.
23. Bridgman, P. C. (1999) *J. Cell Biol.* **146,** 1045–1060.
24. Bi, G. Q., Morris, R. L., Liao, G., Alderton, J. M., Scholey, J. M. & Steinhardt, R. A. (1997) *J. Cell Biol.* **138,** 999–1008.
25. Ren, M., Xu, G., Zeng, J., De Lemos-Chiarandini, C., Adesnik, M. & Sabatini, D. D. (1998) *Proc. Natl. Acad. Sci. USA* **95,** 6187–6192.
26. Hales, C. M., Vaerman, J. P. & Goldenring, J. R. (2002) *J. Biol. Chem.* **277,** 50415–50421.
27. Wilcke, M., Johannes, L., Galli, T., Mayau, V., Goud, B. & Salamero, J. (2000) *J. Cell Biol.* **151,** 1207–1220.
28. Huang, J. D., Brady, S. T., Richards, B. W., Stenolen, D., Resau, J. H., Copeland, N. G. & Jenkins, N. A. (1999) *Nature* **397,** 267–270.
29. Mammoto, A., Ohtsuka, T., Hotta, I., Sasaki, T. & Takai, Y. (1999) *J. Biol. Chem.* **274,** 25517–25524.
30. Zeng, J., Ren, M., Gravotta, D., De Lemos-Chiarandini, C., Lui, M., Erdjument-Bromage, H., Tempst, P., Xu, G., Shen, T. H., Morimoto, T., *et al.* (1999) *Proc. Natl. Acad. Sci. USA* **96,** 2840–2845.
31. Cullis, D. N., Philip, B., Baleja, J. D. & Feig, L. A. (2002) *J. Biol. Chem.* **277,** 49158–49166.
32. Tang, N. & Ostap, E. M. (2001) *Curr. Biol.* **11,** 1131–1135.